

CS 87 17770

ÚSTAV JADERNÉHO VÝZKUMU
ŘEŽ

ÚJV 7857 M

D. Jakeš, J. Rosenkranz

STUDIES IN SOLID STATE IONICS

Report

Řež, January 1987

Informační středisko

NUCLEAR RESEARCH INSTITUTE

ŘEŽ – CZECHOSLOVAKIA

INFORMATION CENTRE

STUDIES IN SOLID STATE IONICS

Dušan JAKEŠ

Jindřich ROSENKRANZ

Řež, October 1986

Studies in solid state ionics

(abstract)

D. Jakeš, J. Rosenkranz

Studies performed over 10 years by the high temperature chemistry group is reviewed. The attention was paid to different aspects of the ionic solids from the point of view of practical as well as theoretical needs of the nuclear technology. This way were studied ceramic fuel compound like uranates, urania-thoria system, solid electrolytes based on oxides and ionic transformations under reactor irradiation.

ÚJV 7857 M

© Nuclear Research Institute - Řež near Prague - Czechoslovakia

Content

1. Nuclear fuel studies	6
1.1. The monouranates of II. a group	6
1.2. Thoria-urania solid solutions	7
2. Solid state sensors for analytical devices	7
2.1. Liquid sodium oxygen meter	7
2.2. Gas oxygen meter	11
2.3. Design of oxygen sensing device for molten steel	11
3. Solid electrolytes studies	14
3.1. Development of the doped thoria ceramic	14
3.2. Zirconia based composition studies	15
4. Melting and transition in ionic solids	15
4.1. Ionic thermometers - general description	15
4.2. Development of the nuclear reactor application	17
4.3. High temperature ITD	19
4.4. Neutron flux level measurements	19
5. Conclusions	20
References	21

C a p t i o n

- Fig. 1. Dependence of the oxygen stoichiometry vs. temperature and partial pressure of oxygen.
- Fig. 2. Design of the oxygen meter (mark 3)
- Fig. 3a. Design of the galvanic cell with brazed doped thoria crucible.
3b. General outlook of the liquid sodium oxygen meter.
- Fig. 4. Scanning microscope image of buried corrosion layer.
- Fig. 5. Corrosion layer grown from depth to surface.
- Fig. 6. Sedimented layer at the electrolyte surface.
- Fig. 7. Sedimented layer after reaction with electrolyte surface.
- Fig. 8. The scheme of gas oxygen meter microfurnace.
- Fig. 9. The scheme of the noise suppressing arrangement of the solid electrolyte galvanic cell for steelmaking.
- Fig. 10. Doped thoria crucible after machining.
- Fig. 11. Schematic view of the electrical conductivity jumps at melting and solidification (heating and cooling curves are marked by the arrows).
- Fig. 12. The sectional view of the modified (with implanted thermocouple) temperature detector.
- Fig. 13. Sectional view of the neutron flux meter.

T a b l e s

Table 1. Tested ionic salts for ITD

Table 2. Boron less glasses for in-pile temperature measurements

Table 3. Comparison of neutron fluences between testing and power station

1. NUCLEAR FUEL COMPONENTS STUDIES

1.1. The monouranates of IIA group /1-8/

The uranates studied in this laboratory earlier has become of practical interest in the industrial use of nuclear energy. The ceramic fuel based on uranium dioxide acquired a principal status as fuel compound in the overwhelming majority of built and commissioned nuclear power stations all over the world. In the course of burning the fission products react mutually and with available uranium as well as liberated oxygen. Thus the uranates of strontium and barium /9/ are formed. That way, the interest in the thermochemistry of this compounds as well as in the analogical compounds of magnesium and calcium has changed from purely academical to technological.

Our work has continued further on in the field of magnesium and calcium uranates /10,11/. The relation between the phase structure and partial pressure of oxygen (P,T functions) was studied.

The magnesium monouranate was examined by transpiration technique /12/ using solid electrolyte oxygenmeter for the oxygen potential control.

The temperature range was 700° - 1200° C. The partial pressure of oxygen was kept by premixed gases /fig.1). The gap in data within $\lg p_{O_2} = 3 \pm 8$ (kPa) of oxygen was caused by technical difficulties to obtain such steady potentials throughout the required time (4 - 10 days). The CO₂ + CO buffer gas made possible to reach steady partial pressures 10⁻⁸ kPa and lower. The miscibility gap formed between two substoichiometric phases has the narrow homogeneity boundaries for MgUO_{4,0} phase and the larger space for pentavalent uranate within composition MgUO_{3,6-3,4}. Another highly substoichiometric phase was found behind the potential gap.

The thermodynamic functions of the MgUO_{4,0-3,9} could not be reliably evaluated because the used technique was not sensitive enough. For the MgUO_{3,6-3,4} phase evaluation has given:

$$\Delta \bar{H}_T = RT \frac{d \ln p_{O_2}}{dT} = - 125.35 \text{ kJ.mol}^{-1}$$

$$\Delta \bar{S}_T = \left(\frac{\partial \bar{G}}{\partial T} \right)_P = + 28.8 \text{ J K}^{-1} \text{ mol}^{-1}.$$

The nearly stoichiometric phase MgUO_{4,0-3,9} was at first analyzed by electron diffraction (monocrystal size 50 nm). The rough monoclinic lattice parameters (in nm) were $a = 0.933$, $b = 0.46$ and $c = 1.00$ $\beta = 93.06^\circ$. The parameters obtained by computer refining with Quinier camera ($\lambda = 0.15405$ nm) and Debye-Scherrer reflexions ($\lambda = 0.15418$ nm) were $a = 0.9337_3$, $b = 0.4579_2$, $c = 1.00156$ nm and $\beta = 93.019_2^\circ$ (st. dev. $\delta a = \pm 0.000084$, $\delta b = \pm 0.000037$, $\delta c = \pm 0.000083$ and $\delta \beta = \pm 0.0079^\circ$). This evaluation has shown more complex structure of nearly stoichiometric MgUO₄, than it was already thought /8,13,14/. Some explanation could be found in the equilibrium time longer by an order than previously used.

The stoichiometry MgUO_{3,6-3,4} brought bigger habitus, due to longer equilibration time in low oxygen potential gas. Still it was not enough to be used in available diffractometer, but too large for electron diffraction (150 kV). By usual refinement of the powder lines reflexions, starting with Bauné Charts was measured the pseudo-hexagonal lattice $a = 0.7331_7$, $c = 1.5202_5$, $\beta = 120^\circ$ (st. dev. $\delta a = \pm 0.00019$, $\delta c = 0.00032$, $\delta \beta = \pm 0.016$ $\lambda = 0.15418$ nm). In all photographs some very weak lines has indicated presence of the superstructure of the extended vacancies. The probable formula of this structure is Mg₂(U^VU^{IV})O₇, which is relatively stable intermediate phase which is followed by further f.c.c. phase Mg(UO₃)₂. In our case, the MgO was finely dispersed in the sample giving no reflexions on uranium background. We were not able to confirm when the precipitation has started, but probably with the formation of the intermediate phase MgUO_{3,6-3,4}, i.e. the real formula have to be Mg_{1-x}UO_{3,6-3,4}.

The determination of the x was not so far carried out..

The analogical study of the calcium monouranate is being completed now.

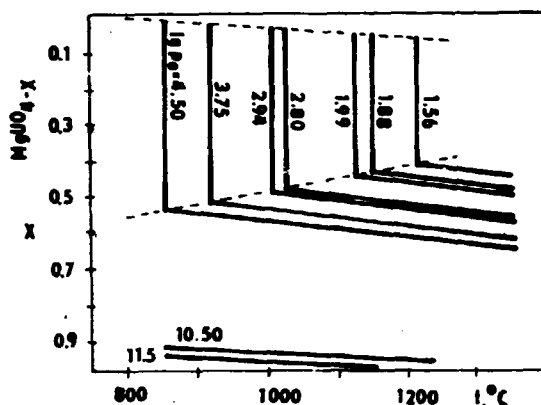


Fig. 1. Dependence of the oxygen stoichiometry vs. temperature and partial pressure of oxygen

1.2. Thoria-urania solid solutions

This system was studied in limited way in the range of urania rich part of the phase diagram (5, resp. 30 mole % of thoria). The phase relations were studied by the transpiration technique at $\log p_{O_2} = -1.68, -2.5, -3.5, -4.5, -5.5, -6.5$ (MPa) within $1100^\circ - 1550^\circ\text{C}$.

The results has shown that at partial pressure of oxygen within -1.6 to -3.6 $\log p_{O_2}$ (MPa) system is analogous to pure UO_{2+x} , where thoria acts as the inert solvent. The final products of the oxidation are U_3O_8 and UO_{2+x} , whose lattice parameters are temperature independent (after annealing). The fluorite lattice alone exists at $\log p_{O_2} = -5.5, -6.5$ (MPa) up to 1250 K in both solid solutions. The co-existence of the orthorhombic U_3O_8 and cubic (f.c.c.) UO_{2+x} was found only at higher partial pressures of oxygen. The orthorhombic phase readily dissolves at 1250 K. In all experiments the intermediate x-ray check-up has confirmed that at given temperature range the meaningful results are obtained only after 72-100 hours of equilibration.

The transpiration results has proved that the oxidation limit is for the whole range of partial pressures $\log p_{O_2}$ from -1.68 to -6.5 , the temperature approx. 1350 K, after which the weight gain has decreased. The shape of the maximum varies slightly with the urania-thoria ratio /%.

2. SOLID STATE SENZORS FOR ANALYTICAL DEVICES

This endcavour was exclusively focused on solid electrolytes conducting by oxygen ion. In other words we have studied some possibilities of doped thoria and stabilized zirconia.

2.1. Liquid sodium oxygen meter

The requirement of the R and D of fast breeder reactors for energy production turned the interest on the necessary controlling and safety devices. One of them was the liquid sodium oxygen meter specified for safeguarding the steam generator against the eventual water-liquid sodium interaction due the corrosive penetration of the stainless steel partition wall.

The studied scheme was the application of the galvanic cell with doped thoria as solid electrolyte. Doped thoria originally suggested by Horseley /16/ was found to be only oxide electrolyte stable enough in liquid sodium for this purpose.

We have tested three different designs /17/ finally accepting the configuration (mark 3) with brazed solid electrolyte (fig. 2). The details of the solid electrolyte (YDT) sensor are on figure 3.

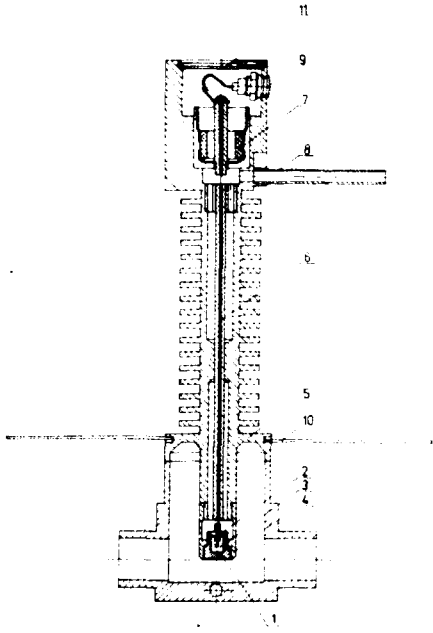


Fig. 2. Design of the liquid sodium oxygen meter (mark 3)

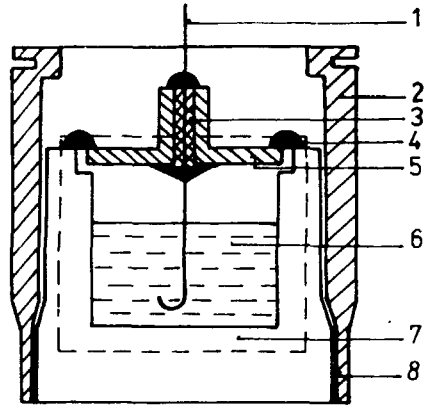


Fig. 3a. Design of the galvanic cell with brazed doped-thoria crucible

- 1 - reversible electrode wire
- 2 - dilasil 97 ring
- 3 - silver brazing
- 4 - glass brazing (t. tr. 800°C)
- 5 - metallic lid
- 6 - reference electrode
- 7 - doped thoria crucible
- 8 - silicateless glass brazing (t. tr. 1350°C)

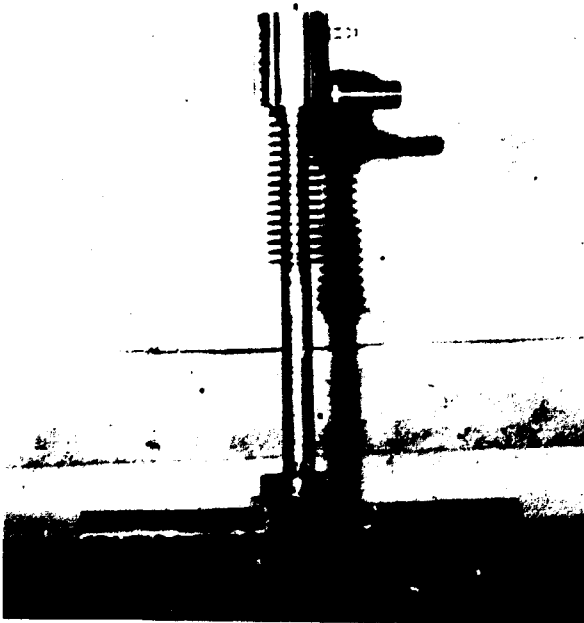


Fig. 3b. General outlook of the liquid sodium oxygen meter

The ceramic electrolyte crucible (thoria with 12 mole % of yttria) was formed the way which makes brazing easier. This particular shape was machined out of sintered pellet as it will be described in section 3.1. The silicateless glass ($\text{CaO} \cdot \text{Al}_2\text{O}_3 \cdot \text{BaO} + 1\% \text{ wt. TiO}_2$) was chosen for brazing because of the best stability against the liquid (450°C hot) sodium. The Ni48-Fe-Cr1 alloy (dilasil 97) was used successfully as its thermal expansion compensates that of thoria and makes good supporting ring. Special problem was the design of a reference electrode. The basic idea was to avoid the high polarisability of the gas or solid electrode by choosing liquid metal co-existence electrode. The Sn + SnO_2 , resp. In + In_2O_3 suspensions were selected from several possibilities. The signal of the indium electrode is the best one, but the high reactivity of liquid indium makes the capping of the electrode space difficult. It requires to cover the inside surface of the nickel lid by thin molybdenum layer (sputtered or vapour-condensated)/17/.

The results /16/ of the e.m.f. measurements has shown that such configuration of the oxygen sensing device has been giving reproducible results with sensitivity limit about 0.5 ppm of oxygen. The cell behaviour agreed to the Nernst equation. The lifetime of the tested galvanic cells spanned from 1600 to 2200 hours with some longer exceptions like 3300 hours etc.

Thereafter the galvanic cells started to lose the e.m.f. and the sensitivity to oxygen. The "infant mortality" was small (1:18).

The surface corrosion layer formed on the solid electrolyte has been deforming e.m.f. in steps. The cell response in comparison with Nernst equation is giving reasonable agreement. The rationalised expression of this equation (for indium electrode) is:

$$\log C_0 \text{ (ppm)} = -1008.5 E / T + 4637/T + C_1 \quad (1)$$

where $C_1 = 3.9973$ calculated from appropriate thermodynamic and solubility data. The readings are deteriorating during the run and developing systematic error, which could be corrected by change of the C_1 for example to 6.9513 after 30 days, 3.9773 after 50 days and 5.6736 after 70 to 120 days of operation in sodium.

So far, we feel that each party of liquid sodium oxygen meters need calibration test. We have used for the check up third law treatment introduced this field by Stavropoulos and Alcock /19/. We have found, that the oxygen dissolution enthalpy came out higher by 22% than the generally accepted value. Still this difference does not fall in the same category with that for air electrode, i.e. more than a twofold deviation. It means that basically the cell electrochemical reaction is well described using equation (1), with time growing by variation the constant C_1 , rather than by altering its slope.

The examination by chemical ceramographic analysis and EDX after testing, has shown several types of damages. The most important is the direct corrosion which could be traced after 1400 hours in a form of islands $20 \mu\text{m}$ under surface (fig. 4). It confirmed the reaction of counter-current fluxes of O^{2-} and Na^+ in the electrolyte. The full layer was formed (grown up to surface) at 3300 hours (fig. 5). The structures identified were Na_2ThO_3 , $\text{Na}_2\text{ThSiO}_5$ and occasionally $\gamma - \text{Na}_2\text{SiO}_5$ (electron diffraction).

Besides this layer another was formed over surface - a sediment (fig. 6). On the picture sediment could be easily recognized as well as piece of free surface from which the sediment has broken away. This occurrence accounts for the random potential fluctuations - the functioning portions of the surface area changing throughout the run.

Part of that sediment could react with electrolyte during the exposure forming new layer (fig. 7) which contains Th and Y in difference to original layer.

As the important problem was recognized the mutual compatibility of the materials creating the reference electrode (i.e. the lid electrode composition, walls, brazing material etc. on fig. 3 the area marked by broken line frame).

Footnote: E is e.m.f. in volts and T absolute temperature in Kelvins.

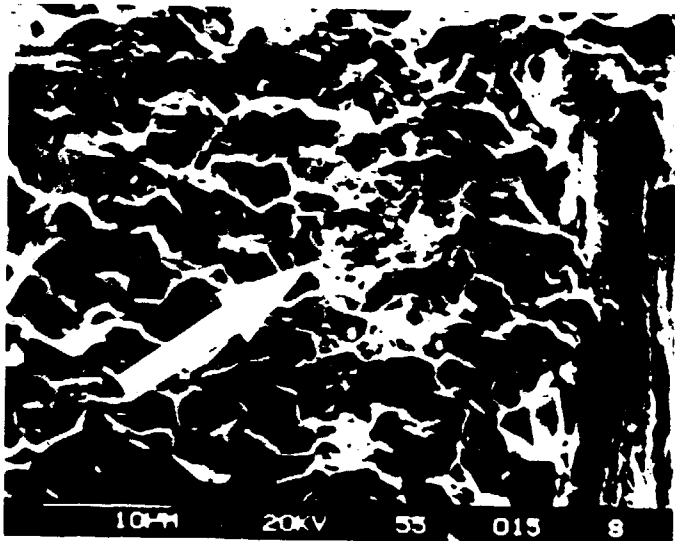


Fig. 4. Scanning microscope image of buried corrosion layer

Fig. 5. Corrosion layer grown from depth to surface

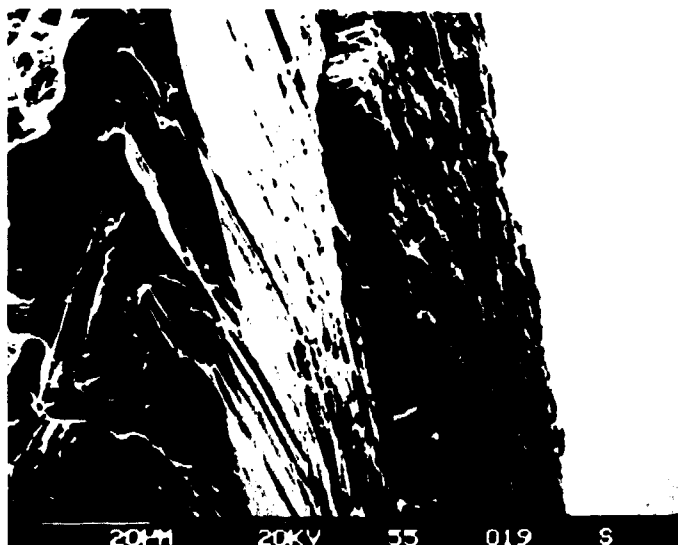


Fig. 6. Sedimented layer at the electrolyte surface

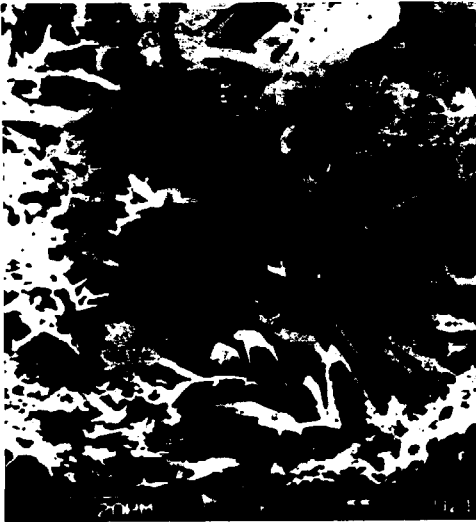


Fig. 7. Sedimented layer after reaction with electrolyte surface

The compatibility and wettability of several lid materials with indium and tin were tested /20/.

Tested compatibility pairs were In-Ni, In-Mo, In-W, In-Nb and In-dilasil 97 (Ni48Fe1Cr) as well as Sn-Mo, Sn-W, Sn-Ta and Sn-dilasil 97. Above those nickel covered by Mo thin layer (200 nm) was tested too. The technique consisted from sessile drop method and metallography extended by EMA technique. The wetting angle was lower than 90° in the case of Ni-In ($77^{\pm}4$ degrees), dilasil and Mo were after 45 minute nearly wetted by indium ($94^{\pm}5$, resp. $99^{\pm}4$ degrees). The same goes for Ni protected by Mo layer ($96^{\pm}4$ degrees). None of mentioned pairs with tin has shown value in the vicinity of 90 degrees.

The experiment in the field of LSOM and namely some effort in the interpretation thermodynamics and compability is still being pursuit and will be published shortly.

2.2. Gas oxygen meter

The solid electrolyte oxygen sensing device for non-pyrolysing gases have been developed and small serie of this instruments was produced recently.

The scheme was based on $0.85ZrO_2 \cdot 0.15CaO$ solid electrolyte tube with closed end ("testing tube" form) produced in Czechoslovakia, which quality was tested in the international experiment of IUPAC /21/. The freely flowing air was used as reference electrode (inside the electrolyte tube). The actual arrangement inside the sensing part (microfurnace working at $700^{\circ}C$) is shown on figure 8. The whole device includes besides the microfurnace an energy block, transformer, temperature controlling and e.m.f. reading systems. The development was mainly done in the field of the availability of necessary parts and materials.

Further miniaturizing in future is under consideration.

2.3. Design of the oxygen sensing device for the molten steel

Within the framework of the development of an oxygen determining instrument for the heavy duty application inside steelmaking furnaces (arc-melting, Siemens-Martin system etc.), we have been studying the question of the electrical noise suppressing measures in solid electrolyte galvanic cell. The quality and possible sources of electrical noise inside the oxygen sensing rig was measured in-vitro in a arc-melting furnace (30 MW).

As a result the arrangement of sensing galvanic cell was suggested as shown on fig. 9 /22/. For the same purpose was the miniature amplifier with flowing zero also developed/23/.

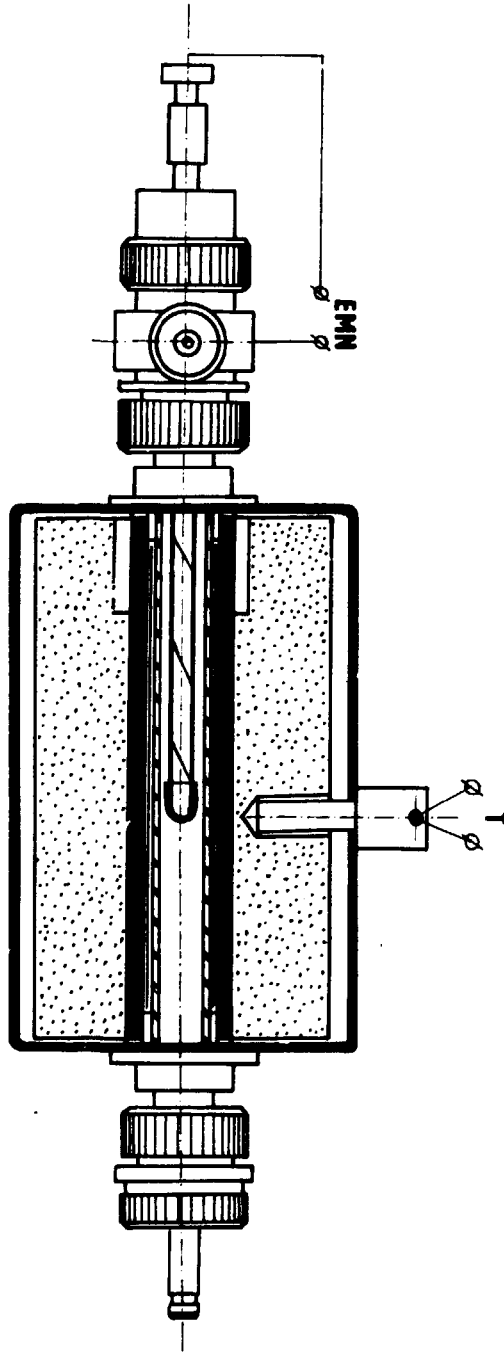


Fig. 8. The scheme of gas oxygen meter microfurnace

The concentration (activity) of oxygen could be calculated by routine way out of the Nernst equation. The signal did not changed if the arc (30MW) was on or out. It seems that was reached the sufficient suppression of the noise.

Steel oxygen meters of that type have been produced on large scale in Czechoslovakia (about 10-15 000 per year) and succesfully used in steelmaking industry.

3. SOLID ELECTROLYTES STUDIES

3.1. Development of the doped thoria ceramic

Our effort was directed to the technology of "liquid sodium grade" doped thoria and its machining into a convinient crucible shape.

The preparation of the powdered doped thoria (12 mole % of yttria) was developed roughly according to Zador /25/.

The solution of thorium and yttrium nitrates with $\text{pH} = 1.6 - 1.7$ has been precipitated by 5 per cent solution of ammonium oxalate ($\text{pH} = 3$ after nitric acid correction). The precipitation has been made at pH up to 2 at room temperature. Mixed oxalates were dried and fired at 1190°C for two hours. The pellets (dia 15 mm, 20 mm high) were pressed in hard metal die and sintered at 1800°C in an argon-hydrogen atmosphere /26, 27/.

Final form of the crucible was machined by diamond tools (fig. 10). The alternative method - ultrasonic drilling was also tested. This technique was found to be less efficient (too many broken pellets), due the inadequate generator (high harmonics). Therefore, the method was abandoned for time being.



Fig. 10. Doped thoria crucible after machining

We have also tested the anticorrosion measures:

- thin layer of crystalized silicateless glass
- increased purify of the doped thoria.

The first technique has reduced corrosion but has changed signal for about 200 mV making the calibration necessary.

The second measure has positive influence, but it is limited in this country by technological possibilities to purify thorium nitrate.

3.2. Zirconia based composition studies

Some studies have been recently in order to prepare ceramic rough material for the sintering of $0.85\text{ZrO}_2 \cdot 0.15\text{CaO}$ solid electrolyte and zircon ($\text{ZrO}_2 \cdot \text{SiO}_2$). For both purposes were employed the coprecipitation of hydroxides at room temperature. The routine decantation, filtration, drying and calcination at $600\text{--}650^\circ\text{C}$ (removal of H_2O residue and NH_4Cl) were used afterwards.

The resulting powder for electrolyte sintering reached specific surface area up to $70\text{ m}^2/\text{g}$ and for syntzircon up to $108\text{ m}^2/\text{g}$ /28/.

The sintering experiment have produced the relative density 98% for the solid electrolyte at 1850°C and 99% for zircon at the temperature 1650°C .

4. MELTING AND TRANSITION IN IONIC SOLIDS

The interest in solid electrolyte science brought the question of the high ionic conductivity of solids created during heating, as highly actual field of inquiry. This became combined with interest in so called ionic thermometers originated in this country (see for example /29/), expanding the range of interest from phase transformation to melting as well.

The main question could be formulated: why some ionic compounds have demonstrated steep-jump-like change of conductivity (into ionic one) at phase transition or at melting, while others have not. Understanding of such effect was important for theory of ionic conduction in ionic solids, as well as for design of the above mentioned ionic thermometers. The process of melting was usually recognized as the one which has been liberating the ionic movement, i.e. causing the conductivity jump /30,31/.

This expectation was not however confirmed experimentally and a new interpretation was formulated by Derrington /33/ and in this laboratory /29,32,34/ (it will be dealt with later).

4.1. Ionic thermometers - general description

(Ionic thermometric detectors - ITD)

Ionic thermometers or more exactly ionic thermometric detectors are discreet temperature detectors. Their performance is based upon the steep conductivity jump (the appearance of ionic conduction at melting or the first - order phase transition of vast number of ionic salts. The idealized melting and solidification conductivity curves (sometimes called Z-conductivity for obvious reason) are shown on figure 11. Usually the actual curves have slightly different slopes for conductivity at melting and at solidification. The ITD sensors were first described by Strnad /29/. The basic design is shown on the figure 12. The detector is actually a simple two electrode conduction cell filled by appropriate ionic salt (HgI_2 for example). The choice of the salt is given by required temperature points (table 1). For non-nuclear purposes the glass bulb is made from borosilicate glass, while for in-pile measurement could be used only boronless glass.

The temperature of the jump is the one of phase transitions or melting depending on the magnitude of the entropy change for an considered process /33,34,37/. The required magnitude of the entropy is more than $20\text{ JK}^{-1}\text{mol}^{-1}$. In the table 1 is shown the case for tested salts. The KIO_3 is an exception, because of the actual process during the jump is not in this case known yet.

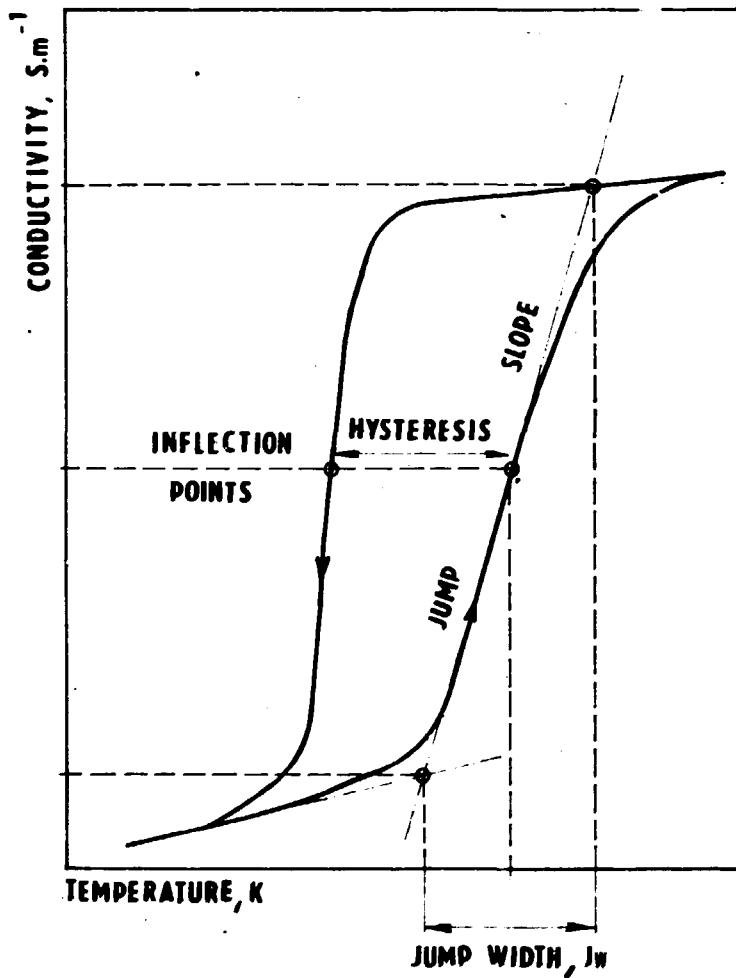


Fig. 11. Schematic view of the electrical conductivity jumps at melting and solidification (heating and cooling curves are marked by the arrows).

Fig. 12. The sectional view of the modified (with implanted thermocouple) temperature detector

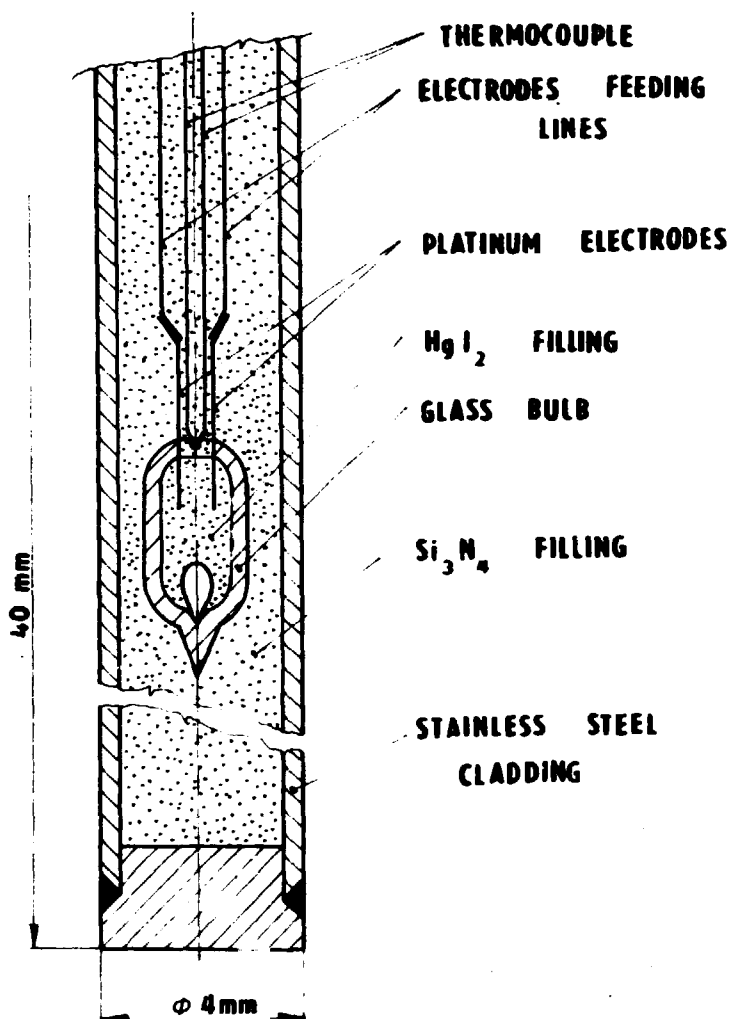


Table 1. Selection of ionic compounds with jumplike change of conductivity (Z-conductivity)

Ionic compound	Transformation temperature $^{\circ}\text{C}$	Transformation type	Transformation entropy $\text{JK}^{-1}\text{mol}^{-1}$
HgI_2	256.0 ± 0.2	melting	35.6
NaNO_3	306.5 ± 0.2	melting	26.0
CdI_2	386.6 ± 0.1	melting	23.5
KIO_3	460.7 ± 0.2	solid - solid	-
CdBr_2	568.3 ± 0.2	melting	180.5
$\text{K}_2\text{Cr}_2\text{O}_7$	395.0 ± 0.2	melting	-
RbI_2	642.5 ± 0.2	melting	24.0

4.2. Development of the nuclear reactor application

The ITD originally specified only for non - nuclear applications were selected as possible in - pile temperature standard. The first irradiation in wet can (1976-79) have shown good stability of the design and especially of the irradiated ionic compounds, thank to isochoric conditions. On the other hand the irradiation in nuclear reactor rig at the working temperature /38/ has shown, that the presence of Loron in the glass bulb makes systematic error about $+18^{\circ}\text{C}$. This kind of deviation could not be well corrected because of several uncertainties connected with it.

Therefore, our interest was directed to general improvement of the reactor radiation field inertness of the actual ITD design.

The selection and eventual correction of the most convenient glass compositions has been made from czechoslovak technical glasses. Selected group of such glasses was irradiated in the wet cell in the WWR-S reactor of the Nuclear research institute, Řež /35/. The whole group of six technical glasses has shown considerable increase in electrical resistivity 2.4 - 5.5 times after fluence $3.0 \times 10^{23} \text{ n.m}^{-2}$ of the fast and $2.0 \times 10^{23} \text{ n.m}^{-2}$ of the thermal neutrons. For the further investigation were used two boronless glasses marked KS - Tasice and Unihost (Table 2).

Table 2. Boronless glasses for in - pile temperature measurements /36/

Type of glass	Content %					
	Na ₂ O	K ₂ O	CaO	SiO ₂	MgO	Al ₂ O ₃
KS Tasice	9.2	5.2	3.8	75.5	0.1	0.2
Unihost	17.8	1.3	5.5	68.6	2.9	3.9

Without boron no systematic error of about mentioned kind was observed. This selection is not final, but ITD made out of both glasses have been successfully used in reactor rig experiments for ITD charged by HgI₂ ($256.0 \pm 0.2 \text{ }^\circ\text{C}$) /39,40/.

The whole ITD assembly (fig. 1) was examined from the point of view of the heat conduction and heat production in the PWR reactor radiation field. The attention was paid to specific participation of all components (canning material, insulating powder, thermocouples, glass, ionic compounds and platinum wires) in the general energy balance /41/. The temperature fields were computed by the finite elements method (230 elements). Three forms of glass bulb were taken to account. The resulting analysis has shown that the influence of the bulb form and type of filling powder were negligible, despite great difference in thermal conductivity coefficients for Si₃N₄ and usual MgO. The influence of boron became nil after 150 days of irradiation. Calculated difference between the water cooled canning surface and the ionic compound compartment was 7.5 °C. Further it will be shown that experimentally found difference is much smaller (about 2.5 times).

The ITD modified for nuclear use (new glass, filling Si₃N₄, with built - in thermocouple) has been tested in fluences comparable to one year in WWR-440 (table 3).

Table 3. Comparison of neutron fluences between testing and power station

Neutron fluence	In experimental WWR-S	Exposition 1 year WWR-440
Thermal neutrons	$2.6 \times 10^{24} \text{ n.m}^{-2}$	$9 \times 10^{24} \text{ n.m}^{-2}$
Fast neutrons	$4.8 \times 10^{24} \text{ n.m}^{-2}$	$4.5 \times 10^{25} \text{ n.m}^{-2}$

The interpreted results has shown that the neutron flux increment has been about $1.5 \times 10^{17} \text{ m}^{-2} \text{ s}^{-1}$ of thermal neutrons and $3 \times 10^{17} \text{ m}^{-2} \text{ s}^{-1}$ of fast neutrons (light water moderation) distorting position of the melting point by heat production for 0.3 centigrade. It could be expressed by the form:

$$t_{op} = t_0 + b \times P \quad (2)$$

here t_{op} is apparent temperature, t_0 is temperature at zero power of the reactor, P denotes actual operating power in MW and b represents decrement $-0.3 \text{ }^\circ\text{C}/\text{MW}$.

The statistically confirmed error in the temperature determination by ITD is $\pm 1.5^\circ\text{C}$ /39,40,42/. Detailed analysis has indicated, that the most important part of the error was caused by the uncertainties in the comparative thermocouples, despite the fact, that all were calibrated against standards before irradiation. The error was not influenced by neutron and photon fluences. The tested ionic charge was HgI_2 and the temperature range during exposure inside the reactor was 250 - 262 $^\circ\text{C}$. Fluctuation was intentional to make the electrical conduction jump repeatedly measurable.

The detailed measurement has shown that the form of the conductivity vs. temperature curves of melting and solidification has not been changed. This indicates that the processes themselves are not influenced as well. Another conclusion could be made that the observed changes (shift of curves position) could be explained by heat production /43/. Described behaviour of the HgI_2 , steep jump uninfluenced by high fluences, makes doubtful the conclusions about purely chemical bond of HgI_2 /44/. High conductivity observed after melting very similar that of simple ionic binary compounds indicates dissociation to Hg^{2+} and I^- rather than creation of big complex ions like HgI^{1+} and HgI_3^{1-} . The mobility could hardly be of the observed magnitude and the kinetics of the complexes formation have to be very high to comply with experiment. Covalent bond would be much more influenced by high photon and neutron flux, than it was experimentally found.

4.3. High temperature ITD

For short period of time some effort was made to develop the ionic thermometers for medium temperatures within 500 - 1000 $^\circ\text{C}$. Some of the ionic compounds were tested /45,37/:

Compounds	Transition melting point $^\circ\text{C}$
SrB_2	640 \pm 1
Na_2WO_4	593 \pm 2
BaCl_2	506 \pm 2
RbI	642 \pm 1
Bi_2O_3	707 \pm 2
KI	679 \pm 2.5

The container material for this temperature range was vitreous silica or alumine tubes with brazen metal electrodes. Silica bulbs only were tested in-pile, which were found satisfactory, if nothing inside the indicated temperature range. Irradiation at low temperature ($\sim 100^\circ\text{C}$) makes silica fragile.

4.4. Neutron flux level measurements

In the course of glass testing for ITD project was found at factorial irradiation experiment that in arrangement (fig. 13) could be measured the neutron level. The measurement should be done as a temperature difference between the hot junction of the thermocouple with glass drop containing some neutron poison (boron) and the hot junction with similar glass without it /45/.

The lifetime of such instrument is given by the speed of burn-up in given neutron flux. Boron glasses are good for rig experiments inside LWR, i.e. up to 100 days. For WWER reactor usual flux level will serve glass with suspension of U^{235}O_2 (1 1/2 year of lifetime). The lifetime vs. sensitivity (energy production decline) is being tested now.

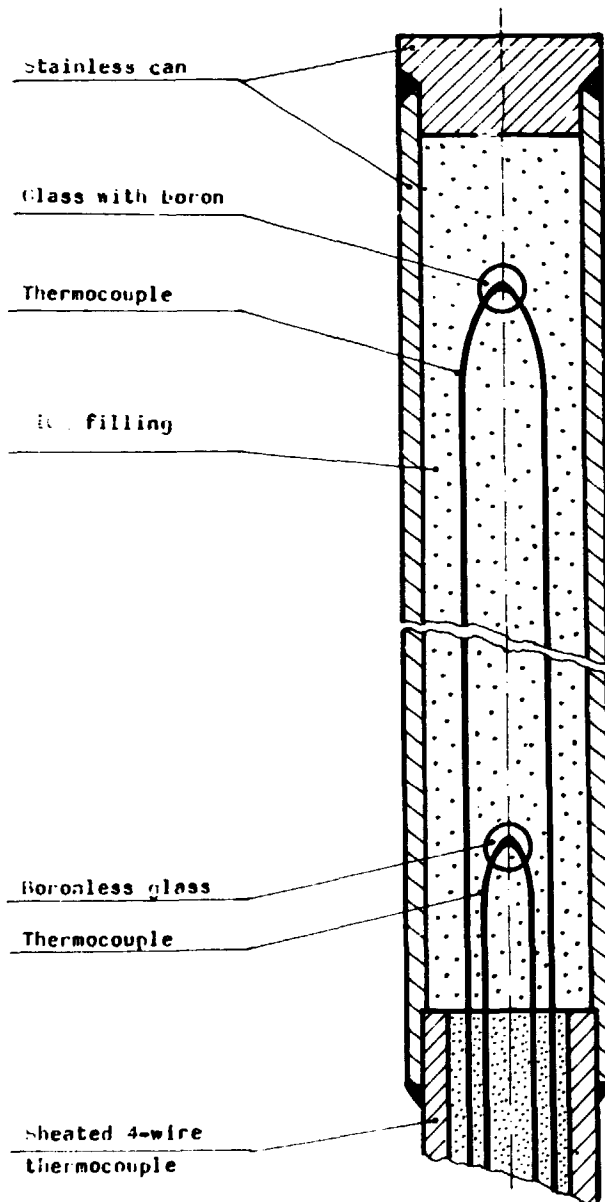


Fig. 13. Sectional view of the neutron flux meter

5. CONCLUSIONS

Solid state chemistry studies in the field of nuclear fuel materials, solid electrolytes, phase transformation were oriented to special needs of nuclear energy production as well as other industrial needs. The last were usually obtained as a fringe benefit of the nuclear research.

The most interesting results were produced in the field of the electro chemical liquid sodium oxygen meter and ionic thermometer (ITD).

REFERENCES

1. H. Landsperský, L. Sedláková, D. Jakeš, J. Appl. Chem. (London) 14, 559 (1964)
2. D. Jakeš, H. Landsperský, L. Sedláková, J. Šulc, Collection Czechoslov. Commun. (Prague) 31, 1677 (1966)
3. D. Jakeš, J. Moravec, I. Křivý, L. Sedláková, Z. anorg. allg. Chemie (Leipzig) 347, 3-4, 218 (1966)
4. J. Klíma, D. Jakeš, J. Moravec, J. Inorg. Nucl. Chem., 28, 1861 (1966)
5. D. Jakeš, V. Schauer, Proc. British Ceram. Soc. 8, 123 (1967)
6. D. Jakeš, L. N. Sedláková, J. Moravec, J. Germanič, J. Inorg. Nucl. Chem. 30, 525 (1968)
7. D. Jakeš, Collection Czechoslov. Commun., 38, 1(1973)
8. D. Jakeš, I. Křivý, J. Inorg. Nucl. Chem. 36, 3885 (1974)
9. S. Imoto, J. Nucl. Mat. 140 (1986) 19
10. D. Jakeš, J. Rosenkranz, Proc. Solid State Chemistry, Karlovy Vary, Czechoslovakia, October 1986
11. D. Jakeš, J. Rosenkranz, Collection Czechoslovak. Commun. (to be published).
12. D. Jakeš, F. Škvor, Silikáty No. 3, 195 (1973)
13. W. H. Zachariassen, Acta Cryst. 2, 788 (1954)
14. W. Rüdorf, F. Pfitzer, Z. Naturforschg, 96, 568 (1954)
15. D. Jakeš, I. Křivý, Collection Czechoslovak Commun. (to be published)
16. G. W. A. Horaeley, UK-AEA, Report AERE-R 3037 (Jan. 1961)
17. D. Jakeš, J. Král, J. Burda, M. Fresl, Solid State Ionics 13, 165 (1984)
18. D. Jakeš, J. Šebková, L. Kubíček, J. Nucl. Mater. 132, 88 (1985)
19. G. Stavropoulos, C. B. Alcock, Canad. Metal. Quart., 10, 257 (1971)
20. D. Jakeš, J. Šebková, L. Kubíček, J. Nucl. Mater. 132, 88(1985)
21. A. M. Anthony, J.F. Baumard, J. Corish, Pure Appl. Chem. 56, 8, 1069 (1984)
22. D. Jakeš, M. Macoszek, V. Lónský, R. Menšík, A. Kokeš, AO 180 800 (Čs. patent) 9.9.1977
23. A. Kokeš, D. Jakeš, AO 177 637 (Čs. patent) 15. 5. 1979
24. Catalogue of the Poldi Steelworks, Kladno 1977
25. S. Zador, Thesis University of London, April 1969
26. D. Jakeš, J. Král, M. Fresl, Report of Nuclear Res. Institute No 5596 A (dec. 1980)
27. D. Jakeš, M. Fresl, K. Svoboda, Report of Nuclear Research Institute No 7534 A (dec.1985)
28. D. Jakeš, E. Kadeřábek, M. Týmpl, Report ÚJV No 7765 Ch, M (June 1986)
29. M. Strnad, Acta IMEKO 1973, B-422, p.227
30. F. D. Richardson in Physical Chemistry of Melts and Metallurgy Academic Press London vol. 1, p.47 (1974)
31. A. R. Ubbelohde in Melting and crystal Structure, Clarendon, Oxford (1965)
32. M. Strnad, Temperature Measurement 1975, Inst. Phys. Conf. Series No 26 (Inst. Phys. London, Bristol 1975), p. 415
33. C. E. Derrington, A. Lindner, O. Keefe, J. Solid St. Chem. 15, 171 (1975)
34. M. Strnad, D. Jakeš, P. Pangrác, Report EGU Tanvald Czechoslovakia (November 1975)
35. D. Jakeš, J. Rosenkranz, J. Král, Silikáty (in english), 28, 195 (1984)
36. D. Jakeš, J. Rosenkranz, M. Strnad, J. Horák, J. Pina, Report ÚJV No 7496-T,A(1985)p.12
37. D. Jakeš, M. Strnad, J. Kott, High Temperatures-High Pressures, 11, 111 (1979)
38. P. Pangrác, Report EGU, No 210 46410262 (1981)
39. D. Jakeš, J. Rosenkranz, V. Krett, M. Strnad, High Temperatures-High Pressure 17, 559(1985)
40. D. Jakeš, J. Rosenkranz, V. Krett, M. Strnad, J. Kott, Rev. Sci. Instrum. 56(12)2319(1985)
41. J. Šik, Report of Škoda Works Ae 5403/Dok (1983)
42. J. Rosenkranz, M. Strnad, D. Jakeš, J. Horák, J. Pina, Report Nuclear Res. Inst. (in Czech) No 7496-T,A (1985), p.20
43. D. Jakeš, J. Rosenkranz, Int. J. Radiation Chemistry and Physics (in press)
44. A. Ubbelohde in Melting and Crystal Structure (Russian translation from Clarendon Press Oxford 1965) Mir Moskva 1963, p. 190
45. J. Rosenkranz, D. Jakeš, Proc. 6th Intern. Conf. Thermodynamics Merseburg Aug.26-29(1980) p. 125 (poster)
46. D. Jakeš, P-Pitterman, J. Rosenkranz, J. Kott, A. Boráková, Čs patent AO 232938 since 26.Oct.1984